

Containerless, low-gravity undercooling of Ti-Ce alloys in the MSFC Drop Tube

M. B. Robinson^a, T. J. Rathz^b, D. Li^c, G. Williams^b, G. Workman^b

^aNASA/Marshall Space Flight Center, Huntsville, Alabama, 35812. (256)544-7774

^bUniversity of Alabama, Huntsville, Alabama, 35899. (256)544-1409

^cNASA/MSFC NRC Resident Research Associate. (256)544-9195

595-29

03-1172

Introduction

Previous tests of the classical nucleation theory as applied to liquid-liquid gap miscibility systems found a discrepancy between experiment and theory in the ability to undercool one of the *liquids* before the L_1 - L_2 separation occurs (1,2). To model the initial separation process in a two-phase liquid mixture, different theoretical approaches, such as free-energy gradient (3) and density gradient (4) theories, have been put forth. If there is a large enough interaction between the critical liquid and the crucible, both models predict a wetting temperature (T_w) above which the minority liquid perfectly wets and *layers* the crucible interface, but only on one side of the immiscibility dome. Materials with compositions on the other side of the dome will have simple surface adsorption by the minority liquid before bulk separation occurs when the coexistence (i.e., binodal) line is reached. If the interaction between the critical liquid and the crucible were to decrease, T_w would increase, eventually approaching the critical consolute temperature (T_{cc}). If this situation occurs, then there could be large regions of the miscibility gap where non-perfect wetting conditions prevail resulting in *droplets* of L_1 liquid at the surface having a non-zero contact angle. The resulting bulk structure will then depend on what happens on the surface and the subsequent processing conditions.

In the past several decades, many experiments in space (5-7) have been performed on liquid metal binary immiscible systems for the purpose of determining the effects that different crucibles may have on the wetting and separation process of the liquids. Potard (5) performed experiments that showed different crucible materials could cause the majority phase to preferentially wet the container and thus produce a dispersed microstructure of the minority phase. Several other studies have been performed on immiscibles in a semi-container environment using an emulsion technique (8,9). Only one previous study was performed using completely containerless processing of immiscible metals (10) and the results of that investigation are similar to some of the emulsion studies. In all the studies, surface wetting was attributed as the cause for the similar microstructures or the asymmetry in the ability to undercool the liquid below the binodal on one side of the immiscibility dome.

By removing the container completely from the separation process, it was proposed that the loss of the crucible/liquid interaction would produce a large shift in T_w and thus change the wetting characteristics at the surface. By investigating various compositions across the miscibility gap, a change in the type and amount of liquid wetting at the surface of a containerless droplet should change the surface nucleating behavior of the droplet – whether it be the liquid-liquid wetting or the liquid-to-solid transition. Undercooling of the liquid into the metastable region should produce significant differences in the separation process and the microstructure

upon solidification. In this study, we attempt to measure these transitions by monitoring the temperature of the sample by optical pyrometry. Microstructural analysis will be made to correlate with the degree of undercooling and the separation mechanisms involved.

Experimental Details

Material Selection and Handling

Because of the limited amount of free-fall/cooling time available in the Drop Tube, a monotectic system had to be found that would provide the necessary critical and invariant temperatures to allow a sample with a reasonable diameter (5mm) to totally solidify. Other considerations were low component vapor pressures at T_{cc} , small oxygen affinity, a known phase diagram, and no toxicity. Not one system met all the requirements. The Ti-Ce (46.8 to 92.0 w/o Ce) system, prepared at the Materials Preparation Center of Ames Laboratory, USDOE, was chosen as the best trade-off. The masses of the samples ranged between 0.34 to 0.43 grams; the calculated, ideally-spherical sample diameters were 5.3 ± 0.2 mm. Drops were opened and stored under inert gas at all times. Oxygen and nitrogen levels within the samples were reported by Ames to be 150-250 ppmw and about 20 ppmw, respectively.

Low-gravity Process

The Drop Tube Facility at NASA/Marshall Space Flight Center (11) was used to provide low-gravity (hereafter labeled 0-g), containerless free-fall conditions. The 0-g samples were processed by electromagnetic (EM) levitation and heating at a frequency of 450 kHz. Once the sample was molten, the power to the coil was automatically turned off and the material allowed to freeze while in free-fall. At the bottom of the Drop Tube, the samples were funneled directly into a thick-walled pyrex tube where they were sealed under a partial pressure of inert gas. The Tube was backfilled with Ti-gettered 5-nines pure He-6% H_2 gas to a pressure of 89.5 kPa. The calculated maximum g-level induced by the drag on the sphere was 25 milli-gravity's.

An eight channel, 125 MHz per channel, 12-bit resolution data acquisition unit was used to monitor silicon detector voltages generated by the brightness of the falling sample. The recalescence temperature of the sample (and thus the amount of undercooling) was calculated knowing the initial release temperature and time ($= 0$), and the final time (t_{rec}) at which recalescence began. Release temperatures were kept to 2023K – 100 degrees above T_{cc} (12). For both the 0-g and 1-g studies, an Ircon Modline two-color pyrometer was used to measure the sample temperature at a rate of 100 readings per second and an accuracy of 1%.

Unit-gravity Process

The 1-g studies were performed atop the Drop Tube Facility in the same EM coil that was used to process the 0-g samples. The samples were levitated and heated to 2023K at which temperature a cooling gas was applied. A typical heating/cooling curve is presented in Figure 1. The samples were released down the Tube to allow the remaining L2 Ce-rich liquid to cool and solidify.

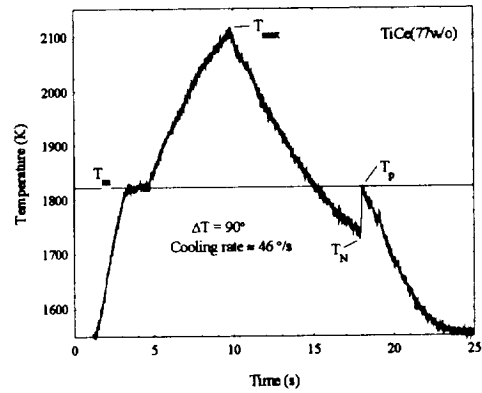


Fig. 1. Typical 1-g sample heating/cooling curve in the EM coil. Temperatures are: T_m , the monotectic, T_p , the recalescence, T_N , the nucleation, and T_{max} , the maximum.

Experimental Results

Undercooling Measurements

Sixty-one 3-nines pure Zr and 23 3-nines Ti were used as melting point calibrations for the optical pyrometer. The average Zr melting temperature was 11 degrees above and Ti was 1 degree above literature values. For the 36 1-g samples processed in the EM coil, the monotectic temperature (T_m) was reproducibly measured from the recalescence peak temperature (T_p) as 1833K with a standard deviation of 19K. From the 34 0-g sample measurements, T_m was reproducibly measured as 1830K with a standard deviation of 7K. Together, the EM coil and Drop Tube processed samples had T_m 's that contrasted to the reported literature value of 1723K (12).

Liquid-to-liquid undercoolings could not be detected with the limited sensitivity of the optical pyrometer. However, Figure 2 shows the liquid-to-solid undercooling measurements placed across the miscibility gap of the Ti-Ce phase diagram. The monotectic line and the binoidal curve have been shifted to account for the measured T_m . A distinct increase in the amount of undercooling achieved in the 0-g samples versus the 1-g samples is observed. The amounts of undercooling could not be controlled in the Drop Tube – if a specimen levitated stably, melted, overheated, and released straight down the Tube without hitting the walls, large undercooling could not be avoided.

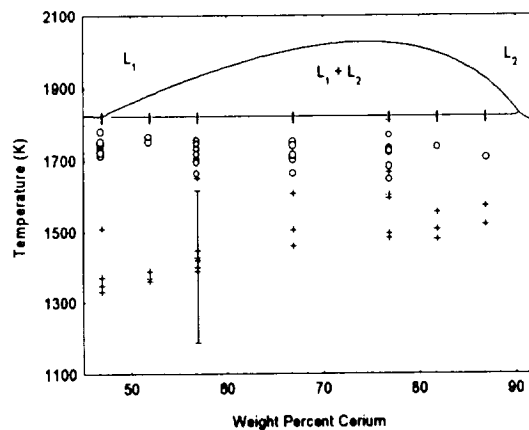


Fig. 2. Immiscibility dome of Ti-Ce phase diagram showing a composite of all the undercooling measurements taken in this study. The 0-g samples (+) showed additional undercooling over the 1-g samples (O) despite the worse-case error bars in the calculated values. The monotectic line and the binoidal curve have been adjusted for the measured T_m values (I).

Microstructure Observations

- 0-g Samples

Fig. 3a shows the general morphology seen throughout the 0-g samples: the size of the large central, concentric β -Ti sphere gets smaller as the volume percent of the Ce-rich liquid increases. At ALL compositions, a Ce-rich layer formed as the outer shell of the sample whose thickness depended on the initial volume fraction of Ce. Secondary Ce droplets were found randomly dispersed in the large β -Ti droplet. No correlation of undercooling to the remaining amount of dissolved Ce contained in the β -Ti matrix could be made.

- 1-g Samples

The 1-g samples are in contrast to the 0-g samples. The 1-g samples show the stirring/shearing effects of the EM field on the β -Ti resulting in large irregularly-shaped globules found near the surface. The Ce droplets in the β -Ti globs is found interdendritically (fig. 3b) and not randomly dispersed as in the 0-g samples. In both the 0-g and 1-g samples, blackish Ce-oxide particles were found sparsely dispersed in both the majority and minority phases.

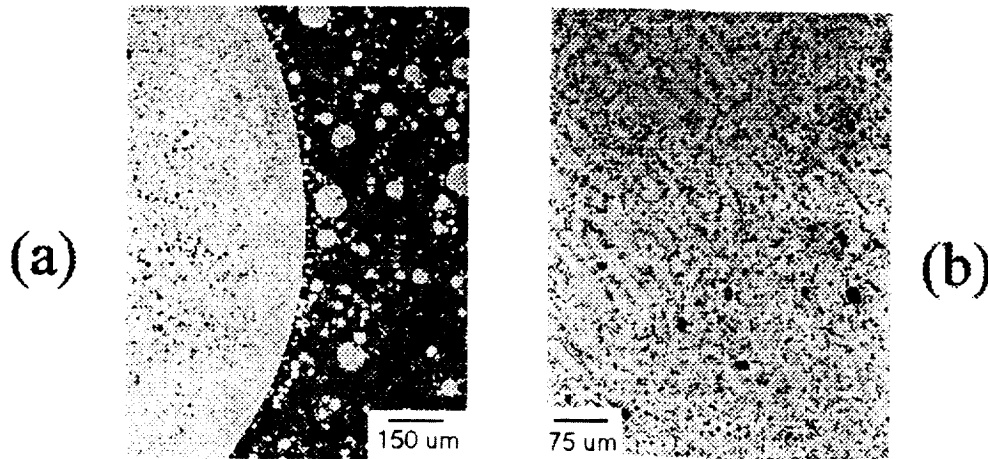


Fig. 3. Photomicrographs of (a) 0-g sample and (b) 1-g sample. The dark phase is Ce-rich and the lighter is β -Ti. Black irregularly-shaped spots are Ce-oxide particles.

Discussion of Results

The large difference in the measured monotectic temperature versus literature values was extensively analyzed. Due to the speed of the pyrometer, the T_p ($= T_m$) of the 1-g EM samples consisted of only 1-2 points and thus had the larger degree of uncertainty. However, the Drop Tube samples' T_m upon heating consisted of the flat

melting isotherm that was very reproducible across the miscibility gap. A flat melting isotherm upon heating implied that the as-cast materials from Ames Laboratories had separated and solidified with a segregated monotectic structure which metallography proved to be correct. Changes in the emissivity due to slight oxidation of the surface should be negligible due to the 2-color signal ratioing of the pyrometer. The oxygen content of the Ti-Ce after processing in the Drop Tube were analyzed by LECO Corporation and are presented in Table 1. About 500 ppmw O₂ was absorbed during the processing of the Ti-Ce in this study. The oxygen content of materials used in previous phase diagram studies (13) could not be found suggesting some inaccuracies in these phase diagrams possibly due to the addition of oxygen.

Table 1. Nitrogen and oxygen content of Zr test drops and TiCe alloys before and after processing in the Drop Tube (in ppmw).

Zr				TiCe			
Arc-melted		After Drop		Before Drop		After Drop	
(LECO)		(LECO)		(Ames)		(LECO)	
O2	N2	O2	N2	O2	N2	O2	N2
1173	7	1235	32	166	18	628	236

The large discrepancy between the 1-g undercoolings and the 0-g undercoolings may be attributable to several things. The 0-g temperatures in this study are a calculated number that depends on thermophysical properties values of the alloy in the undercooled state. A worse-case average error bar of ± 215 K was calculated based on the combined uncertainties of these thermophysical properties. The combined errors would still allow a large number of the Drop Tube undercoolings to be below those of the EM coil samples.

A large difference in cooling rate between the 1-g samples (40K/s) and the 0-g samples (230K/s) may effect the rate of formation of solid β -Ti nuclei and thereby the amount of undercooling. An estimate of this effect can be obtained from a modified form (14) of the classical nucleation theory where the values of ΔG_1^* are based around that given by Kelton (15) of 60kT. At the most, this correction could account for only 10K of additional undercooling.

The relatively quiescent environment of the Drop Tube allowed the 0-g samples to not be stirred as experienced by the 1-g samples in the EM field. The 1-g stirring will sweep the nucleated droplets into much larger spheres by coalescence versus a 0.1 - 2 mm/s calculated Marangoni speed. Without a sweeping effect in 0-g to hasten the coagulation of the droplets, the liquid-liquid dispersion is essentially a high temperature emulsion.

Similar microstructures were seen by Andrews (10) in containerlessly processed Au-Rh samples but only for some of his 10 v/o Au-rich samples. Both Andrews and Perepezko (8) reported a fine dispersion of the minority phase within the majority phase on one side of the miscibility gap and surface wetting of the majority phase by the less-surface energetic minority phase on the other side of the miscibility gap, as predicted by Cahn (3). Approximate calculations of the interfacial energies between the liquids L₁, L₂ and the liquid's vapors indicate that the wetting criteria $\sigma_{L_1L_2} < |\sigma_{L_1V} - \sigma_{L_2V}|$ at the monotectic temperature is easily satisfied. Thus,

the minority Ce-rich phase probably wetted the majority Ti-rich phase in this study, and the minority Ti-rich phase would have formed a dispersion for the Ce-rich side of the dome if not for the lengthy time while undercooled to allow coalescence. Similar results were found by Robinson (16) in 1-g processed Co-Cu metastable immiscibles. A quiescent, 0-g environment with direct non-contact temperature measurements could help eliminate some of the questions regarding these processing effects.

References

1. B. E. Sundquist and R. A. Oriani, *Trans. Faraday Soc.* **63**, 561 (1967).
2. R. B. Heady and J. W. Cahn, *J. Chem. Phys.* **53**(3), 896 (1973).
3. J. W. Cahn, *J. Chem. Phys.* **66**(8), 3667 (1977).
4. Gary F. Teletzke, L. E. Scriven, and H. Ted Davis, *J. Colloid Interface Sci.* **87**(2), 550 (1982).
5. C. Potard, AIAA paper no. 79-0173 (1979).
6. S. H. Gelles and A. J. Markworth, *AIAA Journal* **16**, 431 (1978).
7. T. Carlberg and H. Fredriksson, *Met. Trans.* **11A**, 1665 (1980).
8. J. H. Perepezko, C. Galup, K. P. Cooper in Materials processing in the Reduced Gravity Environment of Space (Guy Rindone, ed., Elsevier Science Pub. Co., Amsterdam, 1982), p. 491.
9. N. Uebber and L. Ratke, *Scripta Metall.* **25**, 1133 (1991).
10. J. B. Andrews, C. J. Briggs, and M. B. Robinson in *Proc. 7th European Symposium on Materials and Fluid Sciences in Microgravity* (Oxford, UK, ESA SP-295, 1989), p. 121.
11. T. J. Rathz, M. B. Robinson, W. H. Hofmeister, R. J. Bayuzick, *Rev. Sci. Instrum.* **61**(12), 3846 (1990).
12. Binary Alloy Phase Diagram (T. B. Massalski, ed., ASM 2nd edition, 1990).
13. E. M. Savitskii and G. S. Burkhanov, *J. Less-Common Metals* **4**, 301(1962).
14. A. J. Rulison, W.-K. Rhim, R. Bayuzick, W. Hofmeister and C. Morton, *Acta. Mater.* **45**(3), 1237(1997).
15. K. F. Kelton, Solid State Physics (F. Seitz and R. Frederick, ed., Academic Press, Inc. 1991), p75.
16. M. B. Robinson, D. Li, T. J. Rathz, and G. Williams, submitted to *J. Mater. Sci.*